Influence of Ni_xMn_{1-x} thickness and composition on the Curie temperature of Ni in Ni_xMn_{1-x}/Ni bilayers on $Cu_3Au(001)$

M. Erkovan[*,1], Y. A. Shokr[2], D. Schiestl[2], C.-B. Wu[2¶], W Kuch[2]

[1]*Sakarya University, Materials Science and Engineering Dept., 54687, Sakarya, Turkey.*

[2]*Institut für Experimentalphysik, Freie Universität Berlin, Arnimalle 14, 14195 Berlin, Germany.*

We present a magneto-optical Kerr effect study of epitaxial bilayers consisting of Ni and Ni_xMn_{1-x} on $Cu_3Au(001)$. The bottom Ni layer, the Ni_xMn_{1-x} layer thickness and its chemical composition were changed and the Curie temperature of the system determined. We focused on two different regimes of Ni_xMn_{1-x} composition, namely a Mn-rich with x between 0.25 and 0.5, and a Ni-rich with x around 0.7. In these two composition ranges, a Ni_xMn_{1-x} overlayer exhibits a different effect on the Curie temperature of the Ni layer. While Mn-rich Ni_xMn_{1-x} layers reduce the Curie temperature of the Ni underlayer, Ni-rich Ni_xMn_{1-x} layers enhance the Curie temperature with respect to the pure Ni film. This is attributed to changes in the effective thickness of the Ni layer by exchange interactions with the Ni_xMn_{1-x} overlayer.

[*]Corresponding Author: merkovan@sakarya.edu.tr

[¶]present address: Chung Yuan Christian University, 200 Chung Pei Rd., Chung Li City, Taiwan 32023, R.O.C.

1. Introduction

Antiferromagnetic (AFM) materials are fundamental components for spintronic applications [1]. In particular, they have found wide usage in connection with the exchange bias (EB) effect discovered in the 1950s [2] to define a reference magnetization direction to the ferromagnetic (FM) layer [3]. Spintronic applications are based on the EB effect of various AFM layers such as CoO [4], NiMn [5,6], FeMn [7], IrMn [8] etc. However, technological applications demand some additional properties from AFM materials, such as high blocking temperature, good corrosion resistance, and high exchange-bias fields. NiMn is one of the AFM materials which satisfy these demands [9]. The spin frustration at the interface is a key in determining the overall magnetic properties of FM/AFM systems [3, 6, 10]. For binary alloy AFM materials like NiMn, this frustration may also depend on the alloy composition. In this study, we have investigated the magnetic properties of epitaxial Ni_xMn_{1-x}/Ni bilayer film systems in two different concentration regimes of Ni_xMn_{1-x} (x between 0.25 and 0.5, "Mn-rich", and x around 0.7, "Ni-rich"). We focused on the variation of the Curie temperature T_C of the ferromagnetic Ni layers during the initial stages of deposition of a Ni_xMn_{1-x} overlayer. We find an opposite behavior in the two concentration regimes, pointing towards a strong dependence of interfacial spin frustration on the alloy composition of NiMn.

2. Sample Preparation

All experiments were performed in an ultrahigh-vacuum chamber pumped to a base pressure of < $3x10^{-10}$ mbar. The chamber was designed both for thin film preparation and magnetic characterization. Electron-beam evaporators were used for the deposition of Ni and Mn. on a $Cu_3Au(001)$ single crystal surface. The Ni_xMn_{1-x} chemical composition x was analyzed by Auger electron spectroscopy (AES). Magnetic hysteresis loops of the samples were taken by in-situ magneto-optical Kerr effect (MOKE) measurements. The growth and structure of ultrathin epitaxial Ni_xMn_{1-x} films on $Cu_3Au(001)$ is discussed in another paper [11].

Before growth of the samples, the substrate was cleaned by Ar^+ sputtering (1–2 keV) and annealing at 800 K for 15 minutes. The sputtering and annealing sequence was repeated until sharp medium-energy electron diffraction (MEED) image was observed. Ni and Ni_xMn_{1-x} layers were grown by (co-)evaporation from high-purity metal rods (99.999% for Ni, 99.99% for Mn) at room temperature (RT). The film thickness was controlled by in-situ MEED. A typical deposition rate was ~1 atomic monolayer (ML)/min. More details can be found in Ref. [5].

3. Results and Discussion

Since the purpose of this paper is to study the influence on T_c of Ni/Cu_3Au(001) of a top Ni_xMn_{1-x} layer also for different Ni thicknesses, it is important to first determine the dependence of T_c on the thickness of the Ni layer. T_c can be determined by temperature-dependent measurements of hysteresis loops by MOKE. Figure 1 shows the temperature dependence of hysteresis loops for 9.6 ML Ni/Cu_3Au(001), taken in longitudinal and polar geometry. The coercivity decreases with increasing temperature, where coercivities in the longitudinal geometry are around 2 times bigger than in the polar geometry. This indicates that the easy axis of magnetization is out of plane. We define T_c as the temperature at which we cannot see any hysteresis loops (coercivity H_c=0), determined by a linear fit of H_c as a function of T. The values of T_c of Ni/Cu_3Au(100) as a function of Ni thickness are shown in Fig. 2. Similar to Ni/Cu(100) [12- 14], there is a spin reorientation transition (SRT) from in-plane to out-of-plane easy axis of magnetization with increasing Ni thickness also in Ni/Cu_3Au(001) [6,15]. We observe an SRT at around 8 ML Ni thickness in Ni/Cu_3Au(001). This higher SRT thickness compared to Ref. [15] could be due to a smoother growth of the Ni film and a concurrently later start of the onset of misfit dislocations.

We turn now to the change in T_c of the Ni layer while depositing NiMn on top. This change depends on the Ni/Mn ratio. We will first focus on Ni-rich Ni_xMn_{1-x} films.

3.1 Ni-rich Ni_xMn_{1-x} samples

Ni-rich Ni_xMn_{1-x} films were prepared at 68, 71, and 74% Ni concentrations. The bottom Ni layer thicknesses were 8.2, 9.6, and 12.6 ML. The dependence of T_c of these films on Ni_xMn_{1-x} thickness is shown in Fig. 3. For these Ni concentrations and Ni_xMn_{1-x} thicknesses the NiMn is paramagnetic at or above RT [16]. We observe that T_c increases slightly during the initial stages of growth of Ni_xMn_{1-x} on top of Ni, and partly relaxes back towards the initial value as the Ni_xMn_{1-x} thickness is further increased. We attribute this to a ferromagnetic polarization of Ni_xMn_{1-x} at the interface to Ni. This polarization increases the effective thickness of the Ni layer in the case of Ni-rich samples in the first few monolayers of Ni_xMn_{1-x} due to the fact that NiMn is paramagnetic at this concentration. We illustrate this in the sketches of Fig. 4. Upon deposition of Ni_xMn_{1-x}, the effective Ni thickness first increases, as shown in Fig. 4 (b), where the entire Ni_xMn_{1-x} layer is ferromagnetically polarized. For larger

Ni_xMn_{1-x} thicknesses, the polarization is saturated at only the interface, as shown in Fig. 4 (c), which leads to a slight reduction in the effective thickness. A very similar behavior of induced ferromagnetic polarization has been observed by photoelectron emission microscopy (PEEM) in FeMn on Co [17]. Due to finite-size effects a change in the effective thickness of the Ni layer is accompanied by a respective change of T_C.

3.2 Mn-rich samples

In order to investigate the effect of Mn-rich Ni_xMn_{1-x} layers, we prepared films with 25, 43, and 48% Ni concentrations. The bottom Ni layer thicknesses were 7.9 and 10 ML. The top NiMn layer thicknesses were varied from 1.5 to around 10 ML. Fig. 5 shows the effect of the Ni_xMn_{1-x} layer on T_C of the Ni layer as a function of Ni_xMn_{1-x} thickness. The behavior found here is opposite to that in the Ni-rich concentration regime. T_c is clearly reduced with increasing Ni_xMn_{1-x} layer thickness. Discussing the effect again in terms of an effective Ni thickness, the deposition of Mn-rich Ni_xMn_{1-x} consequently leads to a reduction of the effective Ni thickness. Due to the tendency of Mn for antiferromagnetic exchange interaction, Mn-rich Ni_xMn_{1-x} films could lead to partial non-ferromagnetic behavior of some of the topmost Ni atoms of the Ni layer, possibly enhanced by intermixing at the interface. This is schematically depicted in Fig. 6. Upon initial deposition of Ni_xMn_{1-x}, the effective Ni thickness slightly decreases by enhanced fluctuations of topmost Ni atoms interacting with Mn of the Ni_xMn_{1-x} layer, as shown in Fig. 6 (b). Since the antiferromagnetic ordering temperatures are higher for Mn-rich Ni_xMn_{1-x}, antiferromagnetic order sets in within the range of thicknesses probed here [6], and the Ni_xMn_{1-x} layer orders antiferromagnetically at higher thicknesses, as schematically shown in Fig. 6 (c). We attribute the steps in the T_C vs. Ni_xMn_{1-x} thickness curves around 3–4 ML for $Ni_{25}Mn_{75}$ and around 7 ML for $Ni_{48}Mn_{52}$ to the onset of antiferromagnetic order in the respective Ni_xMn_{1-x} overlayer. A similar influence of antiferromagnetic order on the transition between paramagnetic and ferromagnetic in an adjacent FM layer has been reported for FeMn/Co bilayers [10].

4 Conclusions

In conclusion, we have observed a change in the Curie temperature of a Ni layer on $Cu_3Au(001)$ induced by the presence of a Ni_xMn_{1-x} overlayer and its dependence on the bottom Ni layer thickness, the ratio of NiMn composition, and NiMn thickness. Mn-rich overlayers cause a lowering of the Curie temperature, which is attributed to the tendency for antiferromagnetic order of Mn. In contrast, the Curie temperature slightly increases for Ni-rich overlayers, which is probably a consequence of induced ferromagnetic order in Ni_xMn_{1-x}

close to the interface with Ni. All of these interpretations are related to direct Ni–Ni, Ni–Mn, and Mn–Mn exchange interactions. A higher number of Ni–Ni interactions in the vicinity of the interface with the ferromagnetic Ni layer would increase the Curie temperature of the latter, while a higher number of Ni–Mn interactions decreases T_C.

Acknowledgement

Mustafa Erkovan would like to thank The Council of Higher Education Turkey (YÖK) for financial support during his stay in Berlin. Yasser Shokr would like to thank the DAAD for support.

1. S. A. Wolf, D. D. Awschalom, R. A. Buhrman, J. M. Daughton, S. von Molna´r, M. L. Roukes, A. Y. Chtchelkanova, and D. M. Treger, Spintronics: A Spin-Based Electronics Vision for the Future Science 294, 1488, 1488-1495 (2001).

2. W. H. Meiklejohn and C. P. Bean, Phys. Rev. New Magnetic Anisotropy 105, 1413 904–913 (1957).

3. J. Nogués and I. K. Schuller, J. Magn. Magn. Mater., Exchange bias, 192, 203 203–232 (1999)

4. E. Demirci, M. Öztürk, E. Sınır, U. Ulucan, N. Akdoğan, O. Öztürk, and M. Erkovan, Thin Solid Films Temperature-dependent exchange bias properties of polycrystalline PtxCo1 − x/CoO bilayers, 550, 595–601 (2014).

5. M. Y. Khan, C.-B. Wu, M. Erkovan, and W. Kuch, J. Appl. Phys. Probing antiferromagnetism in NiMn/Ni/(Co)/Cu3Au(001) single-crystalline epitaxial thin films, 113, 023913, 1-7, (2013).

6. M. Y. Khan, Chii-Bin Wu, S. K. Kreft, and W. Kuch J. Phys.: Condens. Matter, Concentration- and thickness-dependent magnetic properties of NixMn100–x in epitaxially grown NixMn100–x/Ni/(Co/)Cu3Au(001) 25, 386005-1–11 (2013)

7. F. Offi, W. Kuch, and J. Kirschner, Phys. Rev. B , Structural and magnetic properties of Fe x Mn 1-x thin films on Cu(001) and on Co/Cu(001), 66, 064419 1–10 (2002)

8. S. K. Mishra, F. Radu, S. Valencia, D. Schmitz, E. Schierle, H. A. Dürr, and W. Eberhardt, Phys. Rev. B Dual behavior of antiferromagnetic uncompensated spins in NiFe/IrMn exchange biased bilayers, 81, 212404, 1-4, (2010).

9. Y. Wu, “Nano spintronics for data storage,” in: Encyclopedia for Nanoscience and Nanotechnology, edited by H. S. Nalwa (American Scientific, Valencia, CA, Vol. 7, p. 493, (2003),.

10. C. Won, Y. Z. Wu, H. W. Zhao, A. Scholl, A. Doran, W. Kim, T. L. Owens, X. F. Jin, and Z. Q. Qiu, Phys. Rev. B Studies of FeMn/Co/Cu(001) films using photoemission electron microscopy and surface magneto-optic Kerr effect, 71, 024406, 1-5, (2005).

11. W. A. A. Macedo, P. L. Gastelois, M. D. Martins. W. Kuch, J. Miguel, and M. Y. Khan, Phys. Rev. B Growth, structure, and magnetic properties of epitaxial NixMn100-x single layers and Co/NixMn100-x bilayers on Cu3Au(100), 82, 134423, 1-8, (2010).

12. M. Farle, B. Mirwald-Schulz, A. N. Anisimov, W. Platow, and K. Baberschke Phys. Rev. B, Higher-order magnetic anisotropies and the nature of the spin-reorientation transition in face-centered-tetragonal Ni(001)/Cu(001)55, 3708-3715, (1997).

13. W. Kuch, J. Gilles, S. S. Kang, S. Imada, S. Suga, and J. Kirschner, Phys. Rev. B Magnetic circular dichroism microspectroscopy at the spin-reorientation transition in Ni(001) films, 62, 3824–3833 (2000).

14. R. Vollmer T. Gutjahr-Löser, J. Kirschner, S. van Dijken, and B. Poelsema, Phys. Rev. B Spin-reorientation transition in Ni films on Cu(001): The influence of H2 adsorption 60, 6277-6280, (1999).

15. A. Braun, B. Feldmann, and M. Wuttig, J. Magn. Magn. Mater., Strain-induced perpendicular magnetic anisotropy in ultrathin Ni films on Cu3Au(0 0 1) ,171, 16–28 (1997).

16. P. Pal, R. Banerjee, R. Banerjee, A. Mookerjee, G. C. Kaphle, P. Mitra, A. K. Majumdar, and A. K. Nigam, Phys. Rev. B, Magnetic ordering in Ni-rich NiMn alloys around the multicritical point: Experiment and theory, 85, 174405, 1-12, (2012).

17. F. Offi, W. Kuch, L. I. Chelaru, K. Fukumoto, M. Kotsugi, and J. Kirschner, Phys. Rev. B , Induced Fe and Mn magnetic moments in Co-FeMn bilayers on Cu(001), 67, 094419, 1-8 (2003).

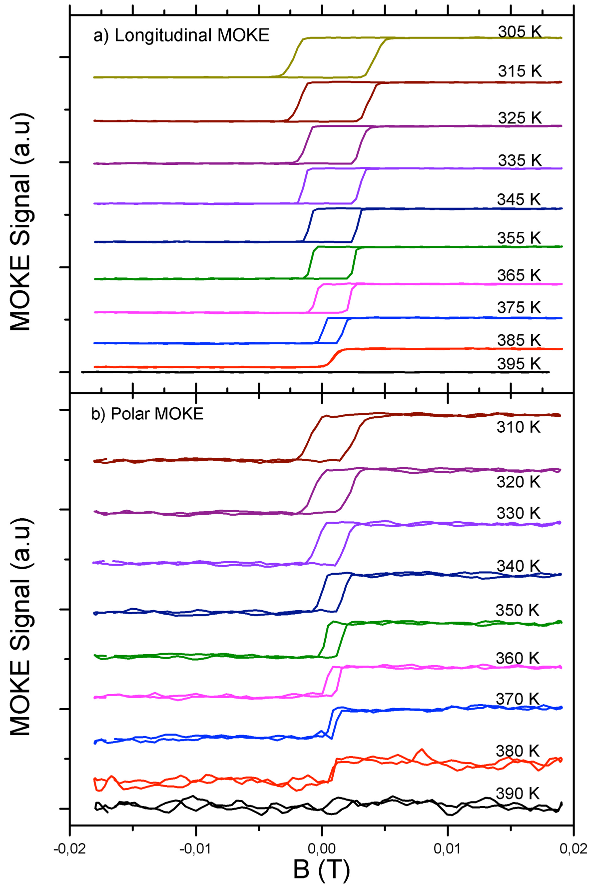

Fig. 1. Temperature-dependent MOKE hysteresis loops of 9.6 ML Ni/Cu_3Au (001) taken (a) in a longitudinal and (b) in a polar geometry.

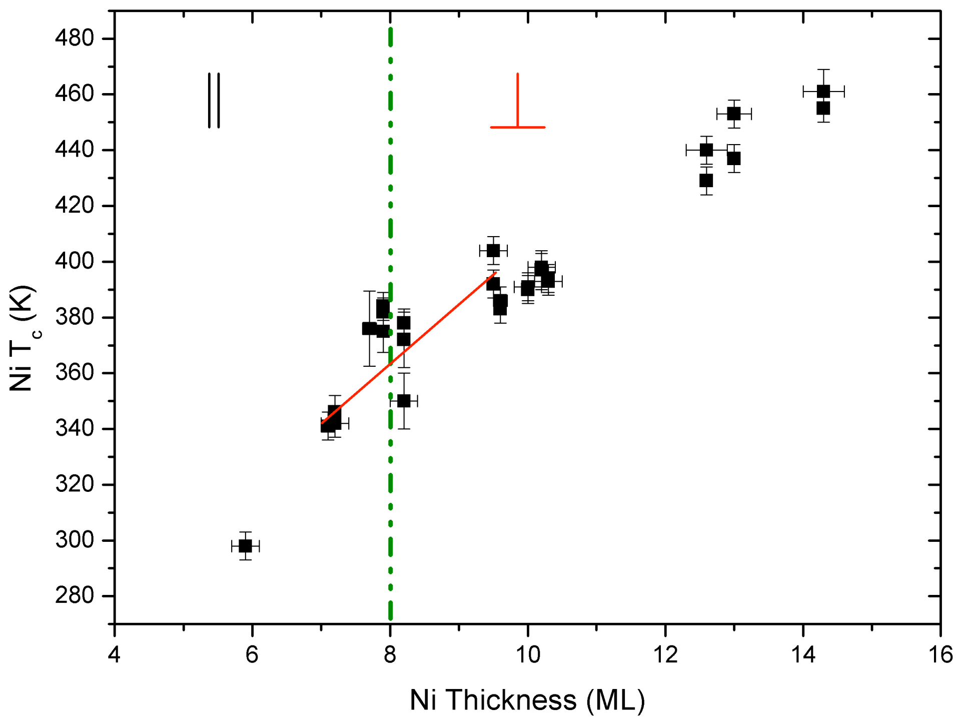

Fig. 2. Curie temperatures of Ni/Cu_3Au (001) as a function of Ni thickness. The dashed line marks the SRT around 8 ML Ni thickness. The red straight line is a linear fit from 7 to 10 ML used to correlate the Curie temperature variation in NiMn/Ni bilayers to a change of the effective Ni thickness.

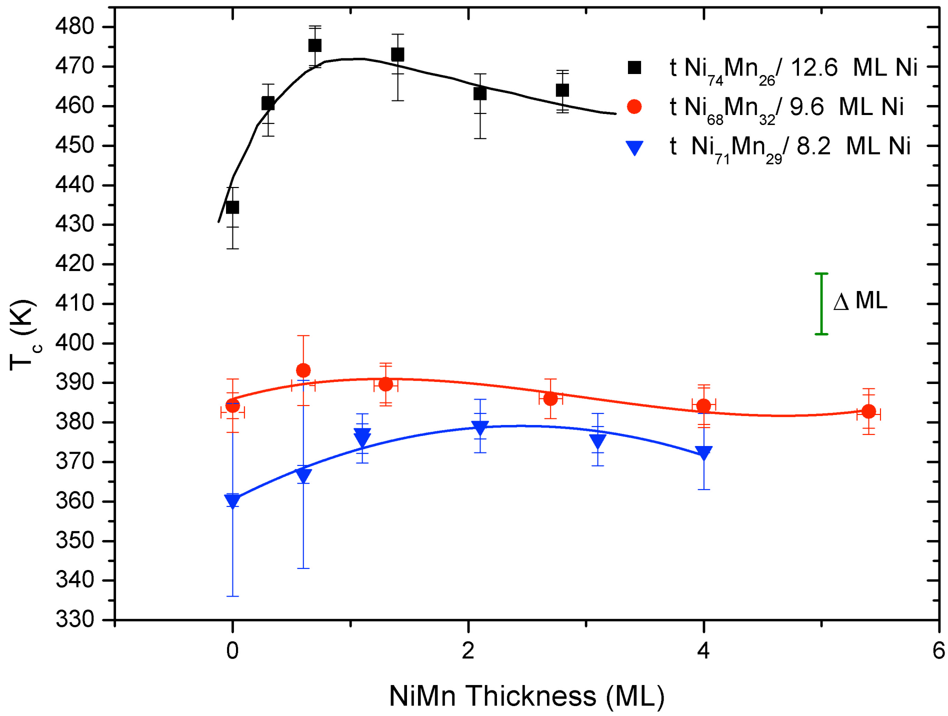

Fig. 3. Ni Curie temperature as a function of the Ni_xMn_{1-x} thickness at different Ni concentrations in the Ni-rich regime. The green scale bar at the right indicates the difference in Curie temperature corresponding to a 1 ML change of the effective Ni thickness estimated from the linear fit in Fig. 2.

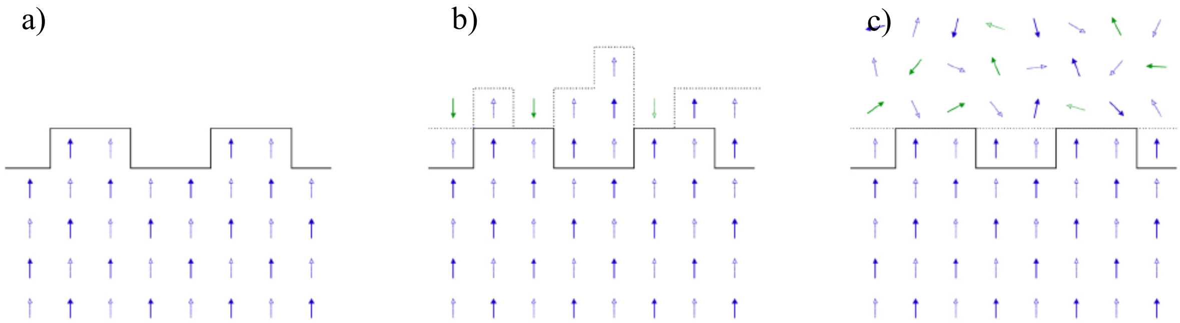

Fig. 4. Schematic model for the Ni Curie temperature changes as a function of the Ni_xMn_{1-x} thickness in the Ni-rich regime. (a) Ni layer, (b) thin layer of Ni_xMn_{1-x} on top, (c) thicker Ni_xMn_{1-x} layer.

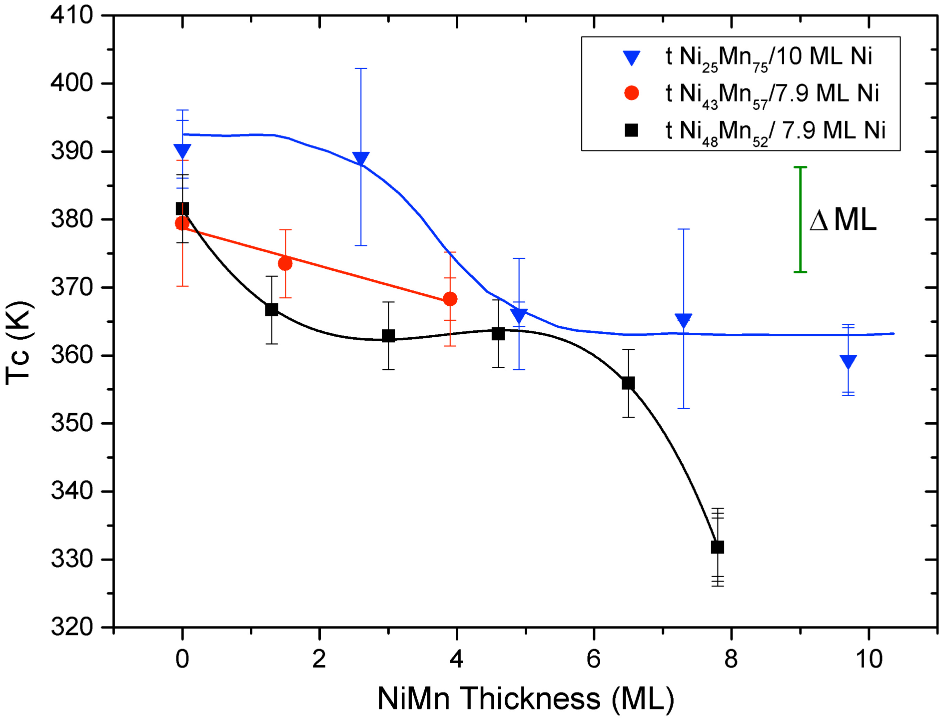

Fig. 5. Ni Curie temperature as a function of the Ni_xMn_{1-x} thickness for different concentrations in the Mn-rich regime. The green scale bar at the right indicates the difference in Curie temperature corresponding to a 1 ML change of the effective Ni thickness estimated from the linear fit in Fig. 2.

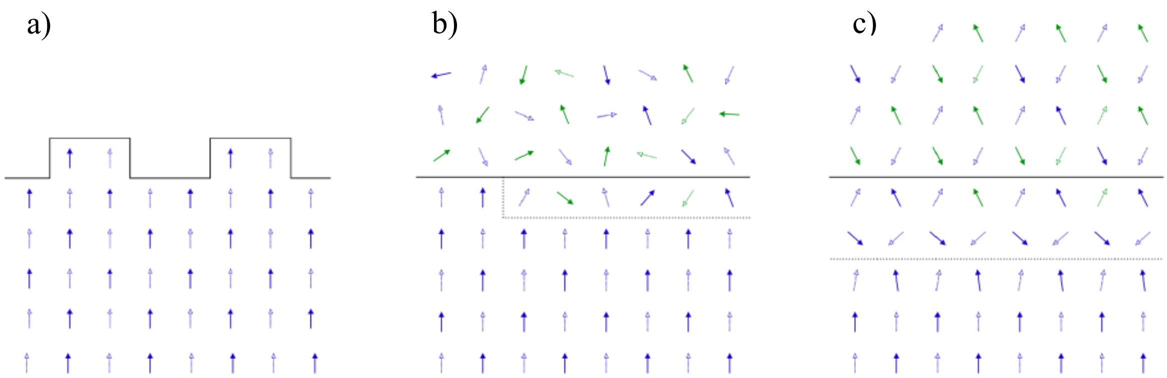

Fig. 6. Schematic model for the Ni Curie temperature changes as a function of the Ni_xMn_{1-x} thickness in the Mn-rich regime. (a) Ni layer, (b) thin layer of Ni_xMn_{1-x} on top, (c) thicker layer of Ni_xMn_{1-x} with antiferromagnetic order.